

# Size Measurement of Radioactive Aerosol Particles in Intense Radiation Fields Using Wire Screens and Imaging Plates

Yuichi Oki<sup>1,\*</sup>, Toru Tanaka<sup>2</sup>, Koichi Takamiya<sup>1</sup>, Naoyuki Osada<sup>3</sup>, Shinnosuke Nitta<sup>2</sup>, Yoshihiro Ishi<sup>1</sup>, Tomonori Uesugi<sup>1</sup>, Yasutoshi Kuriyama<sup>1</sup>, Masaaki Sakamoto<sup>1</sup>, Tsutomu Ohtsuki<sup>1</sup>

<sup>1</sup>Kyoto University Research Reactor Institute, Osaka; <sup>2</sup>Graduate School of Engineering, Kyoto University, Kyoto; <sup>3</sup>Okayama University, Okayama, Japan

## ABSTRACT

**Background:** Very fine radiation-induced aerosol particles are produced in intense radiation fields, such as high-intensity accelerator rooms and containment vessels such as those in the Fukushima Daiichi nuclear power plant (FDNPP). Size measurement of the aerosol particles is very important for understanding the behavior of radioactive aerosols released in the FDNPP accident and radiation safety in high-energy accelerators.

**Materials and Methods:** A combined technique using wire screens and imaging plates was developed for size measurement of fine radioactive aerosol particles smaller than 100 nm in diameter. This technique was applied to the radiation field of a proton accelerator room, in which radioactive atoms produced in air during machine operation are incorporated into radiation-induced aerosol particles. The size of <sup>11</sup>C-bearing aerosol particles was analyzed using the wire screen technique in distinction from other positron emitters in combination with a radioactive decay analysis.

**Results and Discussion:** The size distribution for <sup>11</sup>C-bearing aerosol particles was found to be ca. 70 μm in geometric mean diameter. The size was similar to that for <sup>7</sup>Be-bearing particles obtained by a Ge detector measurement, and was slightly larger than the number-based size distribution measured with a scanning mobility particle sizer.

**Conclusion:** The particle size measuring method using wire screens and imaging plates was successfully applied to the fine aerosol particles produced in an intense radiation field of a proton accelerator. This technique is applicable to size measurement of radioactive aerosol particles produced in the intense radiation fields of radiation facilities.

**Keywords:** Particle size measurement, Radioactive aerosol, Diffusion battery, Imaging plate, Proton accelerator

## Original Research

**Received** July 17, 2015  
**Revision** September 19, 2016  
**Accepted** September 24, 2016

**Corresponding author:** Yuichi Oki

Kyoto University Research Reactor  
Institute, Kumatori, Sennan-gun,  
Osaka 590-0494, Japan  
Tel: +81-72-451-2481  
Fax: +81-72-451-2622  
E-mail: oki@rri.kyoto-u.ac.jp

This is an Open-Access article distributed under the terms of the Creative Commons Attribution Non-Commercial License (<http://creativecommons.org/licenses/by-nc/4.0>) which permits unrestricted non-commercial use, distribution, and reproduction in any medium, provided the original work is properly cited.

Copyright © 2016 The Korean Association for Radiation Protection

## Introduction

In the Fukushima Daiichi nuclear power plant, FDNPP, accident, huge amounts of radioactive aerosols were released to the environment. Their behaviors in the environment have been studied extensively [1]; however, the formation mechanisms of radioactive aerosols in the containment vessels is not well understood. Understanding of the formation in the vessels is very important to elucidate the behavior of the radioactive aerosols in the environment. A simulation experiment under severe conditions is considered to be effective. In such experiments, size measurement techniques capable of

measuring both number-based and activity-based particle size distributions are useful for the clarification of the formation mechanism [2-4]. In addition, the size measurement technique is also useful for the estimation of internal exposure for radiation workers or members of the public. As the internal dose can be expressed as a function of the size of radioactive aerosol particles [5], the size is very important information for the estimation of internal dose.

In this work, a technique combining a wire screen device and imaging plates is proposed as a convenient technique for size measurement of fine radiation-induced particles, and was applied to measurements of radiation fields in an operating proton accelerator.

## Materials and Methods

### 1. Principle

As aerosol particles in the size range of nm to submicron are much smaller than ordinary screen mesh sizes, most of the particles can penetrate the screen. However, a small proportion of the particles cannot penetrate because of the attachment of the particles on the wire due to the large diffusion constant of the particles [6]. Because the penetration ratio of the particles is expressed as a function of particle size, the size distribution can be calculated from experimentally obtained penetration ratios. Wire screen devices such as the screen-type diffusion battery, SDB [7] and graded screen array, GSA [8] were based on this principle. The SDB is a stack of many pieces of screens of the same roughness, while the GSA consists of several single screens of different roughness.

When aerosol particles penetrate a stack of wire screens, the penetration ratio,  $P$ , can be expressed as follows,

$$P = \frac{A}{A_0} = \int_{-\infty}^{\infty} p(r) \cdot \frac{1}{\sqrt{2\pi} \log \sigma_g} \exp\left\{-\frac{(\log r - \log r_g)^2}{2 \log^2 \sigma_g}\right\} d \log r \quad (1)$$

$$p(r) = \exp\left\{-\sum_i K_i N_{s,i} \left(\frac{f_r}{D_c(r)}\right)^{\frac{2}{3}}\right\} \quad (2)$$

$$D_c(r) = \frac{B_c T}{6\pi r \nu} \left\{1 + A \frac{L_{mfp}}{r} + \frac{L_{mfp}}{r} B \exp\left(-C \frac{r}{L_{mfp}}\right)\right\} \quad (3)$$

where  $A_0$  is the radioactivity concentration of whole aerosol particles and  $A$  is that of the penetrated particles.  $r$ ,  $r_g$ , and  $\sigma_g$  are particle radius, geometric mean radius (cm), and geometric standard deviation of the particles, respectively. In this work, size distribution was assumed to have a log-normal distribution.  $p(r)$  is the penetration ratio for particles of

radius  $r$ .  $K_i$  is a specific coefficient calculated from packing density of the wire screen ( $K_i=57$  for a 100-mesh screen, 115 for a 200-mesh screen, 134 for a 300-mesh screen, and 235 for a 500-mesh screen) [7].  $N_{s,i}$  is the number of screen  $i$  and  $f_r$  is the air flow rate to the wire screen device ( $L \cdot \text{min}^{-1}$ ).  $D_c(r)$  is diffusion coefficient for a particle of radius  $r$ .  $L_{mfp}$ ,  $\rho$ ,  $\nu$ , and  $T$  are the Boltzmann constant, mean free path, viscosity, and density of the gas, respectively.  $A$ ,  $B$ , and  $C$  are Cunningham's correction factors ( $A=1.246$ ,  $B=0.42$ , and  $C=0.87$ ) [9].

### 2. Wire screen device

A wire screen device combining the GSA with the SDB was prepared and was applied to a proton accelerator facility in this work. The stacking order and number of the screens are single 100, 200, 300-mesh screens (Screen Nos. 1-3) and 40 pieces of 500-mesh screens (Screen Nos. 4-43) in the downstream direction. A PTFE membrane filter (Toyo Roshi Kaisha Ltd., Tokyo, Japan; pore size 0.5  $\mu\text{m}$ ) was placed at the end of the stack of screens as a backup filter. The size of the effective area of the screens and backup filter was 42 mm in diameter. To prevent leakage of the sampled air, each piece of screen and a backup filter were sandwiched with O-rings, and were kept in an airtight cylindrical housing.

### 3. Air, irradiation and sampling of the irradiated air

The radiation-induced aerosol particles were produced using an 18-L stainless steel chamber in the 150-MeV fixed-field alternating gradient, FFAG, proton accelerator [10, 11] of the Kyoto University Research Reactor Institute, KURRI. One-mm thick aluminum plates were used as lids for both sides of the chamber. The chamber was installed upstream of the beam dump of the beam extraction line. The aerosol measurement was carried out at a measurement station placed 3 m apart from the chamber as shown in Figure 1. Air in the accelerator room was filtered with a HEPA cartridge filter, and supplied from the measurement station to the irradiation chamber at a flow rate of 8.1  $L \cdot \text{min}^{-1}$ . The relative humidity of the air was 42%. The supplied air was confirmed to be aerosol-free using scanning mobility particle sizer, SMPS (TSI Inc., Shoreview, MN; Model 3080) in advance. The SMPS comprised a differential mobility analyzer, DMA (TSI Inc., Shoreview, MN; Model 3081) and a condensation particle counter, CPC (TSI Inc., Shoreview, MN; Model 3025A). The irradiation chamber was stably irradiated for 1 hour with a proton beam current of 1.8 nA. The proton energy was approximately 120 MeV. The returned irradiated air was intro-

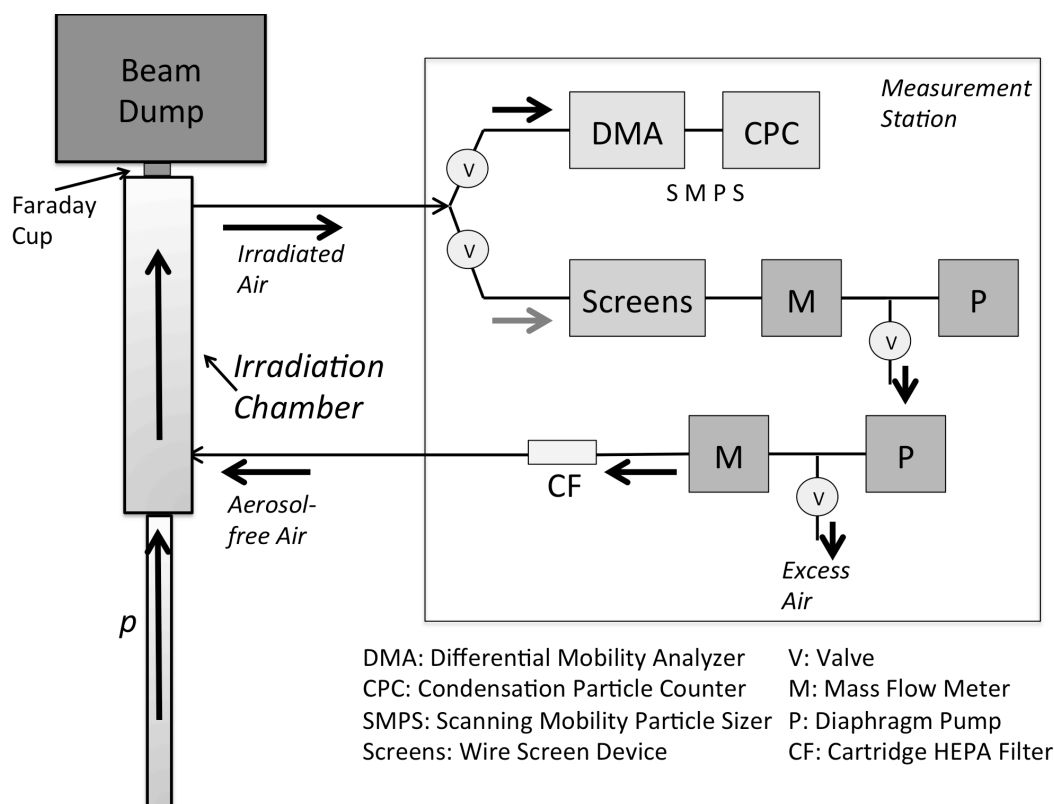


Fig. 1. Arrangement of irradiation chamber and measurement station.

duced to the wire screen device during irradiation at the flow rate of  $7.5 \text{ L} \cdot \text{min}^{-1}$  for size measurement of radioactive aerosol particles. The air was also sampled with the SMPS at a flow rate of  $0.6 \text{ L} \cdot \text{min}^{-1}$  to monitor the number-based size distribution of all of the non-radioactive and radioactive particles.

#### 4. Measurement of size distributions of radioactive aerosol particles

After the sampling of the irradiated air, a radiation image of the 100, 200, and 300-mesh screens, selected pieces of the 500-mesh screens and the backup filter was taken using a large IP (BAS IP MS 3543E, Size  $35 \times 43 \text{ cm}$ ). The IP was exposed for 30 minutes. The exposure was started 20 minutes after the end of the sampling of irradiated air to let a short-lived radionuclide,  $^{15}\text{O}$  (half life: 2 minutes) decay.

Prior to the wire screen experiment, the whole irradiation-induced aerosol particles were collected on the PTFE membrane filter and analyzed with a Ge semiconductor detector system to identify radionuclides in the aerosol. In addition, a separate air irradiation was carried out using a wire screen device with the same screen configuration under the same

beam and sampling conditions in order to estimate contributions from  $^{11}\text{C}$  and  $^{13}\text{N}$  to the intensity of photostimulated luminescence, PSL. Decay curves of radioactivities for selected screen samples and the backup filter were obtained by measurements using GM counter systems (Aloka Co., Mitaka, Tokyo, Japan; GM probe: Model GP-MBR-51, Scaler: Model TDC-105). The selected screen samples were six sets of three pieces of screens (Screen Nos. 4-6, Nos. 11-13, Nos. 18-20, Nos. 25-27, Nos. 32-34, and Nos. 39-41).

In comparison with  $^{11}\text{C}$ , the 478 keV photopeak for  $^7\text{Be}$  was measured for each screen and the backup filter using Ge detectors to obtain a size distribution for  $^7\text{Be}$ -bearing aerosol particles. For each sample, the  $^7\text{Be}$  counts were accumulated for 100,000 s or longer owing to its low activity. The obtained counts were corrected for radioactive decay to the start time of measurement for the first sample.

## Results and Discussion

Large annihilation photopeaks of 511 keV due to positron emitters such as  $^{11}\text{C}$  (half life: 20.39 minutes) and  $^{13}\text{N}$  (9.965 minutes) were observed in the  $\gamma$ -ray spectra of the collected

aerosols. In the spectrum obtained 20 minutes after the end of the sampling, besides the 511-keV peak, photopeaks for  $^7\text{Be}$  (half life: 53.2 days),  $^{24}\text{Na}$  (15 hours),  $^{27}\text{Mg}$  (9.458 minutes),  $^{38}\text{Cl}$  (37.24 minutes), and  $^{39}\text{Cl}$  (55.6 minutes) were observed.  $^7\text{Be}$ ,  $^{11}\text{C}$  and  $^{13}\text{N}$  were produced through (p, xpyn) reactions of  $^{14}\text{N}$  and  $^{16}\text{O}$  in the air including nuclear spallation reactions.  $^{24}\text{Na}$  and  $^{27}\text{Mg}$  were formed from the aluminum lid of the chamber, and  $^{38}\text{Cl}$  and  $^{39}\text{Cl}$  were produced from Ar in the air. Their photopeaks were found to be smaller than approximately 1/1,000 of the 511-keV peak and the PSL intensity is, therefore, considered to be less affected by the nuclides.

The decay curves obtained for the six samples of the selected screens in addition to the backup filter were successfully analyzed by three-component fittings of  $^{13}\text{N}$ ,  $^{11}\text{C}$ , and a longer half-lived nuclide, assumed to be  $^{24}\text{Na}$ . At the start time of the IP exposure, the activity ratios for the screens were estimated to be 73% for  $^{13}\text{N}$  and 25% for  $^{11}\text{C}$  regardless of position in the stacked screens, while the ratio for the backup filter was 61% for  $^{13}\text{N}$  and 38% for  $^{11}\text{C}$ .

Figure 2 shows relative intensities of PSL obtained from the IP image as well as the  $^7\text{Be}$  photopeak for each screen and the backup filter. Each intensity for  $^{11}\text{C}$  was obtained by multiplying the PSL intensity by the activity ratios mentioned above. Particle size for  $^{13}\text{N}$  was not analyzed in this work because the  $^{13}\text{N}$  particle size is difficult to obtain using wire screen methods, owing to an interference of  $^{13}\text{N}$  gas simultaneously formed in the irradiated air. The interference is considered to occur by deposition of acidic  $^{13}\text{N}$  gaseous species on the membrane filters [12, 13] and screen surfaces. The

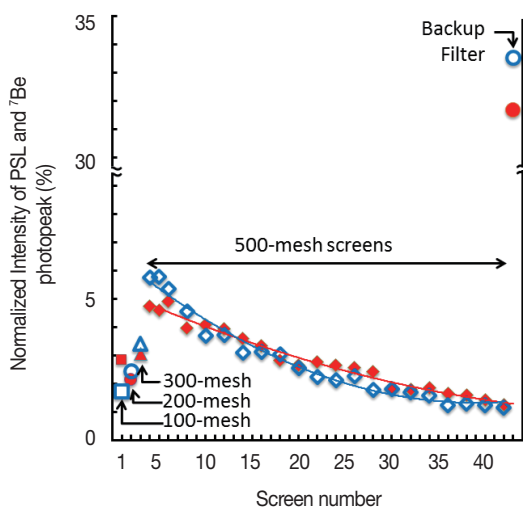


Fig. 2. Intensity of PSL and  $^7\text{Be}$  photopeak for each screen and the backup filter (Closed symbols: PSL, open symbols:  $^7\text{Be}$  activity).

penetration ratio for the  $i$ -th screen was calculated by the dividing total activity of the screens downstream of the  $i$ -th screen and the backup filter by the total activity of all screens and the backup filter. In this calculation, the activity of each 500-mesh screen was estimated by fitting of activity of the measured 500-mesh screen to quadratic equations as shown by the solid lines in Figure 2. Figure 3 shows the obtained penetration ratios for  $^{11}\text{C}$  and  $^7\text{Be}$  as functions of the number of the 100-mesh screen. The number of 200, 300, 500-mesh screens were converted to the number of 100-mesh screens. The converted number of screens was calculated by  $K_i/57 \cdot N_{S,i}$  derived from Equation 2. The solid lines in Figure 3 were obtained by fitting the penetration ratios to Equation 1 using

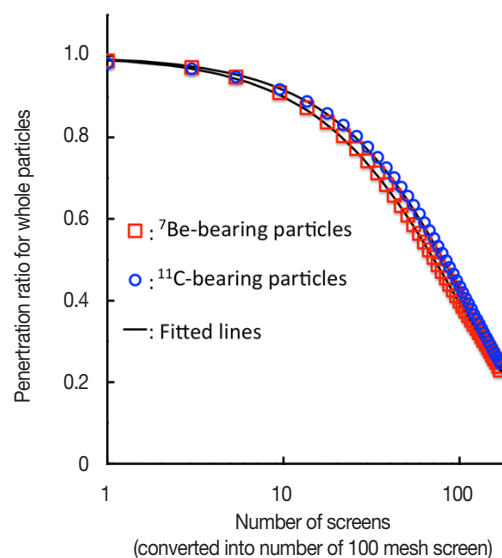


Fig. 3. Relationship between penetration ratio and number of screens.

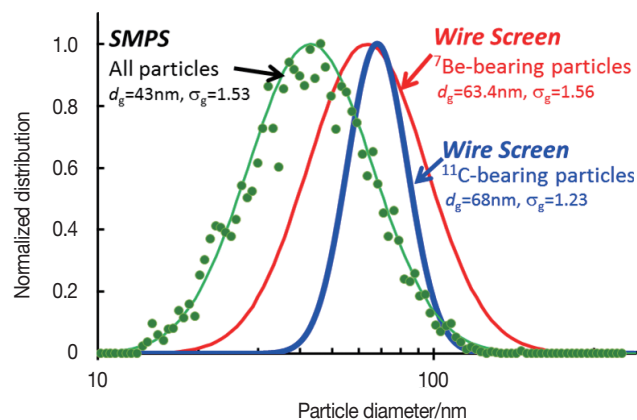


Fig. 4. Activity-based size distributions for  $^{11}\text{C}$  and  $^7\text{Be}$  particles obtained with the wire screen device and number-based distribution obtained with SMPS.

Mathematica.

The obtained geometric mean diameter,  $d_g$ , was 68.0 nm for  $^{11}\text{C}$ -bearing aerosol particles and 63.4 nm for  $^7\text{Be}$ -bearing ones. The geometric standard deviation,  $\sigma_g$ , was found to be  $1.23 \pm 0.02$  for  $^{11}\text{C}$  and  $1.56 \pm 0.01$  for  $^7\text{Be}$ . Figure 4 shows particle size distributions for the radioactive particles (activity-based distributions) along with that of all particles (number-based distribution) obtained by the SMPS. The sizes for the radioactive particles were very close each other, and was larger than that for all particles ( $d_g = 43$  nm) by approximately 20 nm. The radioactive particles are formed by the simple attachment of the radioactive atoms on the non-radioactive aerosol particles. The size difference has been often explained [2, 3, 14] by size dependence of the attachment coefficients [15]. The size distributions can be calculated by multiplying the particle size of the non-radioactive particles by the attachment coefficient for radioactive atoms. Because the attachment coefficient is not constant, and is given as a function of particle size, the calculated size distribution is shifted from the original size of the non-radioactive particles. Endo et al. studied the particle size for  $^{11}\text{C}$  aerosols formed in the tunnel air of a 12-GeV proton synchrotron using SDB [16]. Although the beam intensity was much higher than the FFAG accelerator, the reported particle size, 35 nm in geometric mean radius, is very close to our results, 68 nm in geometric mean diameter. The size may be easily saturated in intense radiation fields.

The IP has an advantage that a radiation image of many samples was obtained by a single exposure; however, multiple radionuclides cannot be distinguished. In this work, the particle size of  $^{11}\text{C}$  was analyzed using IP in distinction from other positron emitters by performing a decay analysis in a separate experiment.

## Conclusion

A particle size measuring method using wire screens and imaging plates was successfully applied to fine aerosol particles produced in an intense radiation field of a proton accelerator. The size distribution for  $^{11}\text{C}$ -bearing-particles was obtained by IP measurement combined with a decay analysis for positron emitters. The geometric mean diameter for  $^{11}\text{C}$  and  $^7\text{Be}$  was found in the range of 60 to 70  $\mu\text{m}$ , and was slightly larger than the non-radioactive particles.

## Acknowledgement

This work was supported by Grant-in-Aid for Scientific Research on Innovative Areas Grant Number 24110009 and JSPS KAKENHI Grant Number 26286076.

## References

1. Kaneyasu N, Ohashi H, Suzuki F, Okuda T, Ikemori F. Sulfate aerosol as a potential transport medium of radiocesium from the Fukushima nuclear accident. *Environ. Sci. Technol.* 2012;46:5720-5726.
2. Kondo K, Muramatsu H, Kanda Y, Takahara S. Particle size distribution of  $^7\text{Be}$ -aerosols formed in high energy accelerator tunnels. *Int. J. Appl. Radiat. Isot.* 1984;35:939-944.
3. Muramatsu H, Kondo K, Kanda Y. Radioactive airborne species formed in the tunnels of a high energy accelerator tunnels. *Appl. Radiat. Isot.* 1988;39:413-419.
4. Kondo K. Radioactive airborne species formed in the air in high energy accelerator tunnels. *J. Nucl. Radiochem. Sci.* 2006;7:R31-R36.
5. International Commission of Radiological Protection. Human respiratory tract model for radiological protection. *ICRP Publication 66.* 1994;24:106-114.
6. Hinds WC. *Aerosol technology: Properties, behavior, and measurement of airborne particles.* 2nd Ed. New York NY. Wiley-Interscience. 1999;160-168.
7. Cheng YS, Yeh HC, Theory of a screen-type diffusion battery. *J. Aerosol Sci.* 1980;11:313-320.
8. Fukutsu K, Yamada Y, Tokonami S, Iida T. Newly designed graded screen array for particle size measurements of unattached radon decay products. *Rev. Sci. Instr.* 2004;75:783-787.
9. Cunningham E. On the velocity of steady fall of spherical particles through fluid medium. *Proc. R. Soc.* 1910;A-83:357-365.
10. Symon KR, Kerst DW, Jones LW, Laslett LJ, Terwilliger KM. Fixed-field alternating-gradient particle accelerators. *Phys. Rev.* 1956;103:1837-1859.
11. Ishi Y, et al. Present status and future of FFAGs at KURRI and the first ADSR experiment. *Proc. of International Particle Accelerator Conference (IPAC' 10).* Kyoto Japan. May 23-28, 2010.
12. Osada N, Oki Y, Yamasaki K, Shibata S. Influence of radioactive gas on particle size measurement of radioactive aerosol with diffusion battery method. *Prog. Nucl. Sci. Tech.* 2011; 1:483-486.
13. Osada N, Oki Y, Kanda H, Yamasaki K, Shibata S, Application of a graded screen array for size measurements of radioactive aerosols in accelerator rooms. *Proc. Radiochim. Acta.* 2011;1:251-255.
14. Oki Y, Kondo K, Kanda Y, Miura T. Aerosol-Size Distribution of Radon Daughter  $^{218}\text{Po}$  in the Accelerator Tunnel Air. *J. Radio-*

- anal. Nucl. Chem. 1999;239:501-505.
15. Lassen L, Rau G. Die Anlagerung radioaktiver Atome an Aerosols (Schwebstoffe). Z. Phys. 1960;160:504-519.
16. Endo A, Oki Y, Kanda Y, Oishi T, Kondo K. Evaluation of internal and external doses from  $^{11}\text{C}$  produced in the air in high energy proton accelerator tunnels. Radiat. Prot. Dosim. 2001;93:223-230.